The effect of sensor shape and number on surface metamerism of colour input devices

Peter Morovič [1] ***and Hideaki Haneishi*** [2,3]
[1] ***Hewlett-Packard Española, Sant Cugat del Vallès, Barcelona, Spain***
[2] ***Frontier Medical Engineering Center, Faculty of Engineering, Chiba University, Chiba, Japan***
[3] ***National Institute of Information and Communications Technology, Tokyo, Japan***

Abstract

Surface reflectances are metameric for a colour input device if they induce identical response under one light source and induce a set of distinct responses under a second light source. Depending on the device sensitivities, metamerism will be different in structure (which reflectances form metamer sets), cardinality (the number of reflectances in each set) and their perceptual magnitude (e.g. the colour mismatch region of a metamer set under a change of illuminant).

In this paper we propose measures to quantify the differences in colour input devices from the point of view of metamerism. Specifically, three quantitative correlates are proposed: the proportion of potentially metameric reflectances (reflectances that give identical response under a canonical illuminant), the proportion of metameric reflectances (potentially metameric reflectances that result in a colour mismatch under any of the test illuminants), the magnitude of the colour mismatch (CIE ΔE's of metameric reflectances under all relevant illuminants). In addition we introduce frequency images that visualise the extent of metamerism for a particular set of spectral sensitivities and a multi–spectral image of interest.

Our aim in this study is twofold: firstly, to provide a means for the study of colour input devices from the point of view of their degree of metamerism; secondly, to expose the relationship between the accuracy of reflectance estimation and the extent of metamerism of a particular device.

To illustrate our approach we compare several devices of various spectral sensitivities (trichromatic and multispectral) as well as series of synthetic sensitivities designed to study two particular aspects: the number of sensors and their shape.

Introduction

Trichromatic colour formation, whereby continuous functions of wavelength describing a surface's colour rendering properties (spectral reflectances) are encoded as three numbers only (the device response), can be thought of as a lossy compression of data. The nature of this encoding process gives rise to the phenomenon of metamerism, whereby reflectances that are spectrally different while inducing identical response for one pair of device and illuminant, induce a set of distinct responses under a change in the device and/or illuminant. The set of metameric reflectances is therefore ambiguous in that there is no direct way to distinguish between each corresponding surface based on the device's responses alone. The reason for this is the discrepancy between the dimensionality of the device (three in the case of trichromatic capture), and the dimensionality of the encoded quantity (a continuous function of wavelength in the case of reflectances). Thus, for a given device response, in theory, there is an infinite set of corresponding surface spectral reflectances – the metamer set.

From literature we know there are differences in how accurately reflectances can be estimated from device responses[2, 3]. These differences lie in the conditions under which the surfaces were recorded (e.g. the recording illuminant), the method employed to perform this estimation (i.e. the algorithm used to extract reflectances from device responses), as well as the device used to record them itself (i.e. device sensitivities). Particularly the first two topics have been of great interest[11, 22, 20, 10, 3, 12]. In terms of the device's spectral sensitivities, it is well known that increasing the number of sensors will reduce the error in estimating reflectances from device responses[1, 7, 13]. Similarly it has been argued that narrow–band sensors are better suited for reflectance estimation[19].

Estimating reflectances from responses amounts to solving two problems: firstly, to discern the transform that occurs at image capture and invert it; secondly, to deal with the ambiguity posed by metamerism that causes this transform not to be uniquely invertible. The majority of reflectance estimation algorithms would assign the same reflectance function to the same response. However, due to metamerism, this response could corresponds to a set of spectrally different reflectances. Depending on the device's spectral sensitivities, the sets of metamers can have large spectral variation. Suppose that was the case, it seems intuitive to label such a device as having a "large extent of metamerism". However, to this date, there is no way to express this notion of the degree of metamerism that a particular set of spectral sensitivities have.

In this paper we propose a number of such measures that formalise this intuition and express it quantitatively. First we introduce three measures: the proportion of potentially metameric reflectances for a particular device and a fixed canonical illuminant; the proportion of the actual metameric reflectances under a change from the canonical illuminant to any one of a set of possible test illuminants; the magnitude in terms of the perceptually related CIE ΔE colour mismatch metric. We also propose *frequency images* as a means to illustrate these measures visually on particular images. These images encode reflectances by assigning their corresponding pixels an intensity value directly proportional to the properties (size) of the metamer set they belong to.

Recently it has been argued that "metamers under one daylight remain metamers under daylights with any correlated colour temperatures"[21], considering the human visual system and blackbody daylight simulators with the ISO/TR16066 Standard

Object Colour Spectra (SOCS) database of spectral reflectances. Another study instead examined the frequency of metamerism from the point of view of the human visual system's ability to identify materials, taking into account the mechanism of chromatic adaptation due to the change in the illuminant[6]. Our approach is new and different in that we look at metamerism from the point of view of colour image capture devices. Given our aim we do not model mechanisms of the human visual system, such as chromatic adaptation and we use a larger set of possible illuminants, beyond the smooth, natural daylights. This enables us to estimate the extent of metamerism in colour reproduction and in it's impact on colour correction, device characterisation, chromatic adaptation and particularly, reflectance estimation – where metamerism is inherently present.

In order to study different devices we need to be able to model their responses of scenes under different light sources. To have this freedom we will use sets of Multi–spectral images of both natural, outdoor scenes[17, 18] as well as images of common, man–made objects[4]. As each pixel in a multi–spectral image is a 31-dimensional wavelength vector, whereby the 31 dimensions correspond to a 10nm sampling between 400nm and 700nm, the images can be rendered under arbitrary illuminant spectral power distributions and arbitrary device spectral sensitivities following the laws of Mondrian–world colour image formation[9]. The multi-spectral images also serve the purpose of the ground-truth of surface spectral reflectances in the process of reflectance estimation.

Analysis

Given a multi–spectral image with spectral reflectances $S_i(\lambda)$, their response vectors can be calculated via the following colour formation equations:

$$r_i^x = \int_\omega R_x(\lambda)E_a(\lambda)S_i(\lambda)d\lambda \tag{1}$$

where r_i^x is the response corresponding to the spectral sensitivity $R_x(\lambda)$ of the i-th reflectance in an image and the integral is taken over the range ω of visible wavelengths, in this case $[400,700]nm$. Denoting $\mathbf{R}(\lambda)$ the matrix of spectral sensitivity functions and $\mathbf{r}_i$ a vector of device responses, we can re-write Eq. (1) as:

$$\mathbf{r}_i = \int_\omega \mathbf{R}(\lambda)E_a(\lambda)S_i(\lambda)d\lambda \tag{2}$$

It can be seen from the colour formation equations in Eq. (2), that there is a discrepancy between the response vector $\mathbf{r}$ and the function of surface spectral reflectance $S_i(\lambda)$ in that $\mathbf{r}$ is a finite–dimensional discrete sampling of the (theoretically) infinite, continuous function $S_i(\lambda)$. Common colour input devices such as cameras, scanners as well as the human visual system, use three channels through which surface reflectance is integrated. For such devices the left hand side of Eq. (2) is a 3×1 vector. On the other hand, reflectances are in practice represented as vector quantities, usually resulting in a 31×1 vector on the right hand side. Thus there are three degrees of freedom on the left hand side, while there are 31 degrees of freedom on the right hand side. More generally, assuming a device with C channels and assuming reflectance is represented in a D dimensional vector space, Eq. (2) is a system of C linear equations of D unknowns. Since $C \ll D$, this system is under–determined and has $D-C$ degrees of freedom (for $C=3$ and $D=31$ the system has 28 degrees of freedom) and it can be shown that for each $\mathbf{r}$ there is an infinite set of possible $S(\lambda)$'s which in colour science are referred to as metameric reflectances[5].

In order to study the frequency of metamerism in multi-spectral scenes we find all sub–sets of reflectances from a multi–spectral image that are metameric. So, for a set of reflectances $S_l(\lambda)$ and their corresponding responses $\mathbf{r}_m$ for a given device with spectral sensitivities $\mathbf{R}(\lambda)$ under illuminant $E_a(\lambda)$, we define the set $\mathscr{P}_{[E_a,\mathbf{r}_m]}$, such that a reflectances $S_k(\lambda)$ is it's member if and only if:

$$\begin{aligned} \forall S_l(\lambda) \in \mathscr{P}_{[E_a,\mathbf{r}_m]} \quad &: \\ |S_k(\lambda) - S_l(\lambda)| \quad &> \quad \varepsilon_S \\ &\wedge \\ |\int_\omega \mathbf{R}(\lambda)E_a(\lambda)S_k(\lambda)d\lambda - \mathbf{r}_m| \quad &< \quad \varepsilon_r \end{aligned} \tag{3}$$

whereby ε_S is a threshold value determining that reflectances $S_k(\lambda)$ are different from all other reflectances $S_l(\lambda)$ already in the set $\mathscr{P}_{[E_a,\mathbf{r}_m]}$ and ε_r is a threshold determining that the response of reflectance $S_k(\lambda)$ is sufficiently similar to the chosen response $\mathbf{r}_m$.

Due to metamerism it is clear that the number of sets $\mathscr{P}_{[E_a,\mathbf{r}_m]}$ has to be $\leq$ the number of all reflectances in a scene. Their number is equal if all reflectances are spectrally distinct and at the same time induce different responses. In practice this is unlikely and most responses of an image will have corresponding sets with more than one member.

The set $\mathscr{P}_{[E_a,\mathbf{r}_m]}$ is thus the set of all spectrally different surface reflectances in an image that, within some set threshold ε_S, induce, identical response under a particular illuminant, within some threshold ε_r. The reflectances in this set however, need not be metameric according to the definition used earlier. Each of the sets $\mathscr{P}_{[E_a,\mathbf{r}_m]}$ has to be examined under a change of illuminant (or device/observer) in order to establish whether the match under $E_a(\lambda)$ is maintained, in which case the effect of metamerism is absent, or if this match breaks, in which case metamerism is exhibited.

Let us assume a set of illuminant spectral power distributions $E_i(\lambda)$ representative of possible light sources (see Figure 3 and 4 below). In order to examine each of the sets of reflectances that induce identical responses under a chosen cannonical illuminant $E_a(\lambda)$, we define the set $\mathscr{Q}_{[E_a,\mathbf{r}_m]} \subseteq \mathscr{P}_{[E_a,\mathbf{r}_m]}$ of reflectances $S_k(\lambda)$ as follows:

$$\begin{aligned} \exists E_i(\lambda) \quad \wedge \quad \exists S_l(\lambda) \in \mathscr{P}_{[E_a,\mathbf{r}_m]} : \\ |\mathbf{r}_k^i - \mathbf{r}_l^i| > \varepsilon_r \end{aligned} \tag{4}$$

where $\mathbf{r}_k^i$ and $\mathbf{r}_l^i$ are responses of reflectances $S_k(\lambda)$ and $S_l(\lambda)$ respectively under illuminant $E_i(\lambda)$ and ε_r is the same threshold value determining whether two responses are significantly different.

If a set $\mathscr{Q}_{[E_a,\mathbf{r}_m]}$ is non–empty then the reflectances within are strictly metameric, otherwise the reflectances in the set $\mathscr{P}_{[E_a,\mathbf{r}_m]}$ are simply spectrally different reflectances that always induce the same response, considering the domain of possible change of test illuminants.

We perform two analyses of the sets $\mathscr{P}_{[E_a,\mathbf{r}_m]}$. Given a multi–spectral image, we express the proportion of reflectances from

the image that are potentially metameric (the number of unique reflectances that induce identical response divided by the total number of unique reflectances). This is a quantitative expression of the potential extent of metamerism. Next we look at the extent of the metameric mismatch, by finding those conditions for which the reflectances result in a colour mismatch. This means finding at least one of the test illuminants for which the unique surfaces that record to identical response under canonical illumination cease to induce identical response and therefore result in a colour mismatch. This is an expression of the magnitude of actual metamerism in a given image.

So as to quantify the mismatch due to metamerism, we then examine the effect of all illuminants on each set $\mathcal{Q}_{[E_a,\mathbf{r}_m]}$ and find all illuminants $E_i(\lambda)$ that cause a non–zero CIE Lab ΔE colour difference among the reflectances in $\mathcal{Q}_{[E_a,\mathbf{r}_m]}$. The CIE Lab ΔE statistics then express an approximation of the perceptual magnitude of metamerism in any given image.

We also introduce *frequency images* – graphical representations of the extent of metamerism for a particular device on a particular multi–spectral image and serve the purpose to illustrate this extent. The *potential metamer frequency images* are gray–scale images that have lightness of a pixel as a function of the cardinality (number of elements) of the corresponding potential metamer set $\mathcal{P}_{[E_a,\mathbf{r}_m]}$.

Analogously, *metamer frequency images* can be defined, having lightness of a pixel as a function of the size (number of elements) of the metamer set $\mathcal{Q}_{[E_a,\mathbf{r}_m]}$. Finally, *colour mismatch frequency images* have lightness as a function of the CIE ΔE statistics. The largest set of reflectances that are potentially metameric/metameric/have the highest colour mismatch will be shown as white pixels in an image at their original spatial locations, the pixels that are uniquely identified by their responses instead will be shown as black pixels at their original spatial locations. Thus, the darker a frequency image, the smaller the extent of metamerism and conversely, the lighter a frequency image, the larger the extent. Thus, a completely white image would correspond to the case whereby no surface can be identified uniquely by a device response, whereas a completely black image would correspond to the opposite case of no metamerism, where all surfaces are uniquely identified. From the point of view of reflectance estimation, the darker the metamerism frequency image the better.

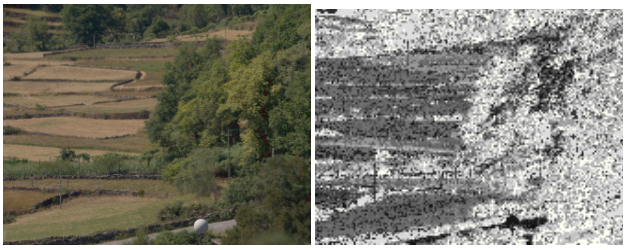

Figure 1. *An example of potential metamer frequency images. The left hand side image is an RGB rendering of the multi-spectral scene and the right-hand side image is a metamer frequency image for a 3-channel RGB camera. The lighter the pixels in the right hand side image, the larger the metamer set it corresponds to.*

For example, the left hand side of Figure 1 shows the sRGB rendering of a multi–spectral scene from the Nascimento *et al.* data set. Considering an RGB camera (with sensitivities plotted in Figure 6 left) and CIE illuminant D65 as the canonical set–up, the right hand side of Figure 1 shows the potential metamer frequency image. The light areas correspond to potential metamer sets that contain large numbers of surface spectral reflectances.

Experimental Set-up

We analyse multispectral images of 16 natural, outdoor scenes[17, 18], the Nascimento set, as well as 24 images of common, man–made objects[4], the UEA set. The images have full spectral reflectance vectors at each spatial location, thus allowing their rendering for arbitrary illuminant spectral power distributions and arbitrary known device spectral sensitivities.

Both data sets of multi–spectral images use a spectral sampling of 10nm steps. The UEA set samples spectra between 400nm and 700nm while the Nascimento set samples between 400nm to 720nm. In this study we use the 400nm to 700nm range at 10nm steps resulting in 31 samples.

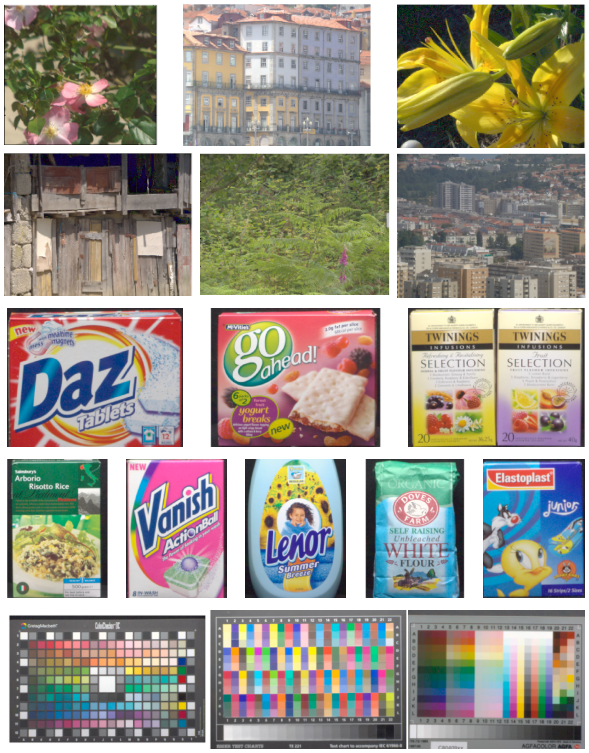

Figure 2. *An example of an sRGB rendering of 6 natural scenes from the Nascimento set (top 2 rows) and 11 scenes from the UEA set (bottom three rows) under illuminant D65. The bottom row of images corresponds to (from left to right) the Macbeth Digital ColorChecker Chart, the Esser Test Chart and the Agfa IT8.7 Chart respectively.*

The Nascimento images are on average of a higher spatial resolution with image sizes at least 680×420 pixels, whereas the UEA set has a smaller pixel count. The UEA set is well documented to have a high degree of spectral accuracy, corresponding to measurements by a telespectroradiometer with a median ΔE of

below 1.2 units[4].

As the canonical set–up we chose illuminant CIE D65, an off–white daylight simulator. Figure 2 shows examples of sRGB renderings from both sets of multi–spectral data under this illuminant. As the set of possible illuminants for which we study the effect of metamerism we use 173 spectral power distributions covering CIE standard illuminants (daylight simulators, incandescents and fluorescents) as well as measured actual light sources (natural and artificial)[8]. Figure 3 shows the spectral power distributions (left), normalised to have a maximum of 1, demonstrating large spectral variation, as well as their corresponding CIE u'v' chromaticities with each illuminant plotted as an sRGB rendering of a perfect white diffuser under that illuminant (right), demonstrating the broad coverage of chromaticities.

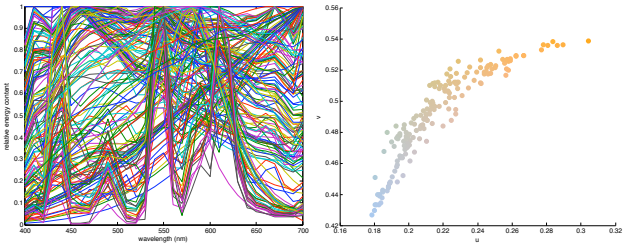

Figure 3. *Illuminant spectral power distributions of 173 illuminants, normalised to have a maximum value of 1 (left) and CIE u'v' chromaticity diagram of the 173 illuminants with the colors plotted corresponding to an sRGB rendering of the respective white points of each illuminant (right).*

We also define the thresholds of accuracy ε_S and ε_r. In the experiments reported here, ε_S is defined such that two reflectances are different if they differ in at least one sampled wavelength when quantised to an integer scale of $[0,100]$, while ε_r is defined such that two responses differ if they differ in at least one of the XYZ channels when quantised to an integer scale of $[0,100]$.

We next summarise the steps taken to quantify the potential for metamerism in an image:

1. **Pre–processing**
   Some images contain margins of uniform black pixels (not displayed in Figures 3 and 4), as well as natural uniform areas in the actual scenes in both sets. For this reason we quantise the reflectances to an integer scale of $[0,100]$ and choose those that are unique in an image (a reflectance is unique if it differs from all other reflectances in an image at at least one sampled wavelength by at least a value of 1). This quantisation corresponds to enforcing the ε_S threshold of spectral difference. The number of these unique reflectances is used as the total number of reflectances in a scene when calculating proportions of metameric surfaces.

2. **Potential Metamers**
   Responses are calculated for the image under the canonical light source (CIE D65) and the particular device spectral sensitivities. The responses are quantised in each channel to an integer scale of $[0,100]$, according to the threshold value ε_r. Only responses that are unique, up to this precision threshold, are considered, and of the unique responses we further consider only those that correspond to more than 0.05% of the number of unique reflectances, in order to avoid potential metamer sets of only a few reflectances.
   Then, for each unique response $\mathbf{r}_m$ we find all reflectances that record to the same response, the number of these is the cardinality of the set $\mathscr{P}_{[E_a,\mathbf{r}_m]}$. This set contains therefore reflectances that are recorded as identical, but have differing spectral reflectances (since we only considered unique reflectances here). So, any reflectance in $\mathscr{P}_{[E_a,\mathbf{r}_m]}$ is a potential metamer.

3. **Metamers**
   Each set of reflectances $\mathscr{P}_{[E_a,\mathbf{r}_m]}$ is then rendered under each of the test illuminants (173 spectral power distributions, plotted in Figure 3). Similarly as above, the responses under each test illuminant are quantised to an integer scale or $[0,100]$, and only those responses are considered that are unique after this thresholding operation. Each reflectance that results in distinct responses under at least one of the test illuminants is a member of the set $\mathscr{Q}_{[E_a,\mathbf{r}_m]}$.
   The set $\mathscr{Q}_{[E_a,\mathbf{r}_m]}$ therefore contains reflectances that are members of $\mathscr{P}_{[E_a,\mathbf{r}_m]}$ (spectrally different, recording to identical response under canonical conditions) while at the same time these reflectances record to different responses under some test condition. Thus, reflectances in $\mathscr{Q}_{[E_a,\mathbf{r}_m]}$ are metamers.

4. **Evaluation**
   We evaluate the metamerism potential in terms of summary statistics of 1) the cardinalities (numbers of members) of the non–trivial sets $\mathscr{P}_{[E_a,\mathbf{r}_m]}$ (sets containing more than 0.05% samples each) in proportion to the total number of unique reflectances – expressing the proportion of potential metamers in an image; 2) the cardinalities of the sets $\mathscr{Q}_{[E_a,\mathbf{r}_m]}$ in proportion to the total number of unique reflectances – expressing the proportion of actual metamers in an image; 3) CIE ΔE colour differences between metameric reflectances under any of the 173 test illuminants for which $\mathscr{Q}_{[E_a,\mathbf{r}_m]}$ is non–empty.

CIE XYZ Colour matching functions

First we show the extent of surface metamerism considering the CIE 1931 Standard Colorimetric Observer XYZ spectral sensitivities in Table 1. (for a detailed analysis see[15]).

	min	mean	median	max
Potential Metamers (%)	21	62	63	100
Metamers (%)	2	13	14	33
Mismatch (ΔE)	0.4	7.8	5.9	94.2

Summary statistics of the proportion of potential metamers, actual metamers and of CIE ΔE colour mismatch errors over all 40 multispectral images for the CIE XYZ spectral sensitivities.

Well over half the reflectances in each of the scenes are members of a non–trivial set $\mathscr{P}_{[E_a,\mathbf{r}_m]}$, and therefore record to an identical response under the canonical set–up. This means that, almost half the reflectances in a scene are unique in that no other reflectances in the scene records to the same response. Of all reflectances, just over 10% in each of the scenes belong to a set

$\mathcal{Q}_{[E_a,\mathbf{r}_m]}$. These reflectances are ambiguous under the reference illuminant and furthermore exhibit a colour mismatch under at least one of the 173 test illuminants. This proportion of actual metamers is significantly smaller than the proportion of potential metamers discussed first.

In terms of the CIE Lab ΔE colour difference measure, considering all pairs of reflectances in the sets $\mathcal{Q}_{[E_a,\mathbf{r}_m]}$ for any of the 173 test illuminants, the colour differences have a mean of $7.8\Delta E$ (the distribution resembling a truncated normal distribution with a peak in the 0 to 5 ΔE interval).

Number of channels

Next we look at the relationship between the number of recording channels and metamerism. In the context of reflectance estimation, it has been shown that increasing the number of sensors results in higher–dimensional responses which in turn increase the accuracy of reflectance estimation[13].

First we use 6 sets of synthetic sensors ranging from 2 to 7 recording channels, with each channel being a delta function (sensitive to a single wavelength). Their sensitivities are designed so as to uniformly sample the range of wavelengths between 400nm and 700nm, thus a two channel device will have two sensors, one peaking at 500nm and the second one peaking at 600nm, a 3 channel device will have three sensors, one peaking at 470nm, the seond peaking at 550nm and the third at 630nm, etc.

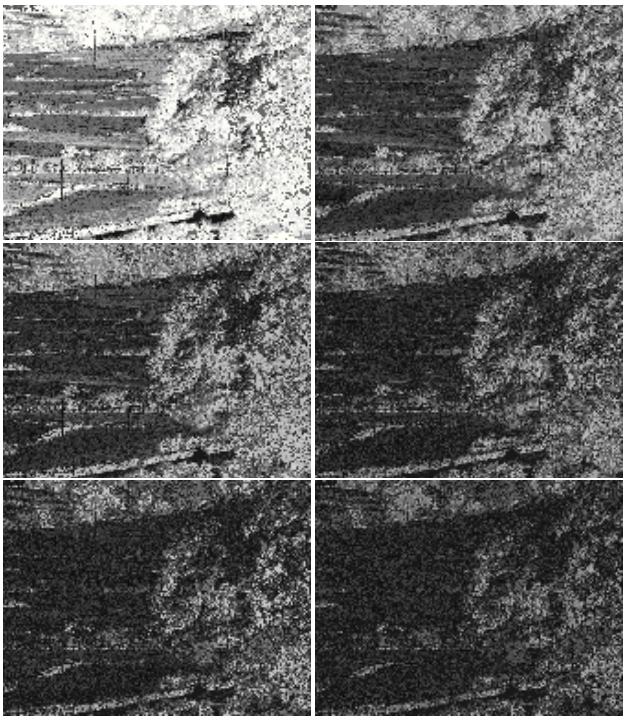

Figure 4. *Metamerism frequency images for theoretical devices with (from top left to bottom right) 2 to 7 narrow band sensors.*

The effect of the number of such sensors can be illustrated on the potential metamer frequency images shown for each of the sensors on one of the scenes from the Nascimento set. The images are ordered from the top left corner to the bottom right corner (left to right) in order of increasing number of sensors. Pixel brightness is directly proportional to the number of reflectances with the same response and it can be seen that as the number of sensors increases so the images become darker and hence less metameric.

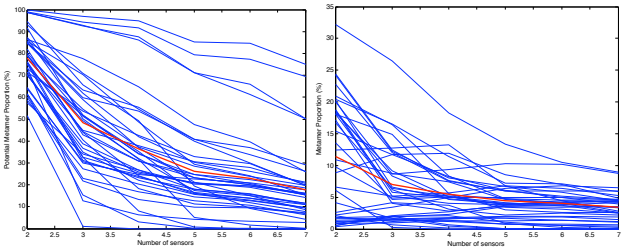

Figure 5. *The % of potential metamers in an image (left) and the % of actual metamers in an image (right) as a function of the number of sensors for each of the 40 multi-spectal images (thin lines) as well as the average (bold lines).*

In Figure 5 we show the relationship between the number of sensors and the % proportion of potential metamers (left) and actual metamers (right) in each of the 40 images (thin blue lines) as well as the average (thick red line). The more sensors are used the smaller the % proportion of potential metamers as well as actual metamers in an image.

Next we look at the difference between the same trichromatic device spectral sensitivities of a SONY RGB camera compared to a 6-band HDTV camera. The spectral sensitivities of both can be seen in Figure 6.

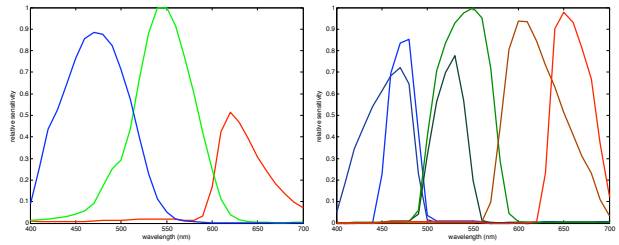

Figure 6. *The spectral sensitivities of a SONY RGB camera (left) and a 6–band HDTV camera (right).*

A study of reflectance estimation has shown that the 6-band HDTV device performs significantly better than the 3 channel RGB camera, reducing estimation error by nearly 50%[13]. In Figure 7 the difference between the two devices can be seen in their potential metamer frequency images. The image corresponding to the trichromatic RGB device (left) is clearly lighter than the image corresponding to the 6-band HDTV device (right).

Table 2 also summarises the potential metamer, actual metamer and colour mismatch statistics. It can be seen that the 6-band HDTV camera has a 37% decrease in terms of the potential metamer proportion and a 45% decrease in the actual metamer proportion. For more details see[14].

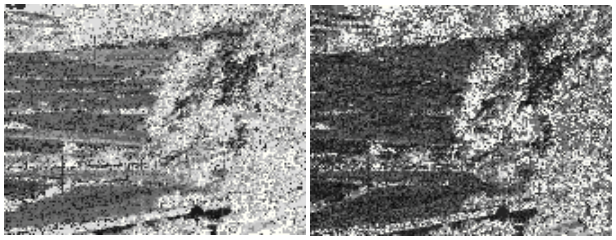

Figure 7. *Potential metamer frequency images for the trichromatic RGB camera (left) and the 6 channel HDTV camera (right).*

	min	mean	median	max
SONY RGB				
Pot. Metamers (%)	29	68	69	100
Metamers (%)	1	11	12	30
Mismatch (ΔE)	0.3	6.1	4.8	94.2
6 band HDTV				
Pot. Metamers (%)	1	43	38	100
Metamers (%)	0	6	5	20
Mismatch (ΔE)	0.4	8.0	6.5	91.1

Minimum, mean, median and maximum statistics of the proportion of potential metamers, actual metamers and CIE ΔE colour mismatch errors for all 40 multi-spectral images tested under 173 illuminant spectral power distributions.

Narrow band vs. Broad band sensors

The shape of the recording sensor sensitivities also plays an important role in the accuracy of reflectance capture and identification. More specifically, the width of support, or whether a sensor is narrow band or broad band, is of particular interest. A study into device's regions of surface spectral reflectance discriminability has suggested that narrow band sensors are better suited for this task[16] and another study into the design of spectral sensitivities for colour array capture also supported this notion[19]. In this section we look at the closely linked question of how the shape of sensors influences the extent of surface metamerism.

We conduct a synthetic experiment to study this dependency, by designing 4 artificial spectral sensitivity sets of a trichromatic device with varying widths of support ranging from 5 wavelengths (narrow band no overlap) up to 17 wavelengths (overlapping broadband) in 4 wavelength increments.

Figure 8 shows the potential metamer frequency images for these four synthetic device spectral sensitivities ordered from top left to bottom right in order of increasing width of sensor support. Again a trend can be seen whereby the top–left image is the darkest and the bottom right image the brightest, suggesting that the broader and more overlapping a device's sensitivities the larger the potential metamer sets.

Figure 9 also shows the relationship between the width of the sensors and the % proportion of potential metamers (left) and actual metamers (right) in each of the 40 images (thin blue lines) as well as the average (thick red line). The wider the sensor support, the bigger the % proportion of potential metamers as well as actual metamers in an image. While there is a clear trend for each of the 40 images, there is large variation as to the magnitude of the actual proportions of potential and actual metamerism for each of the images.

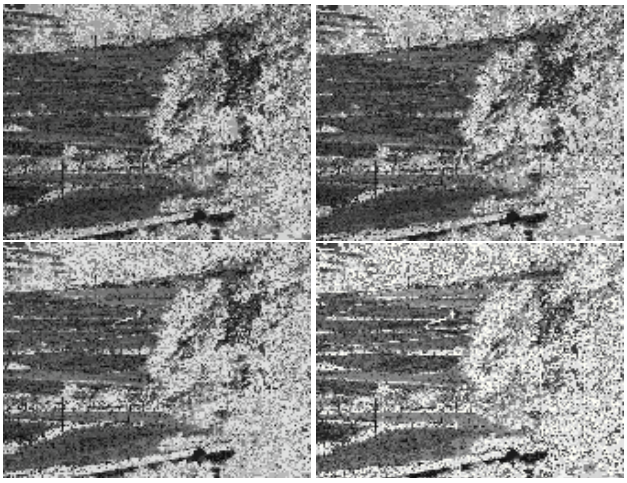

Figure 8. *Potential metamer frequency images for a theoretical device with three sensors of width (from top left to bottom right) 5, 9, 13 and 17 sampled wavelengths.*

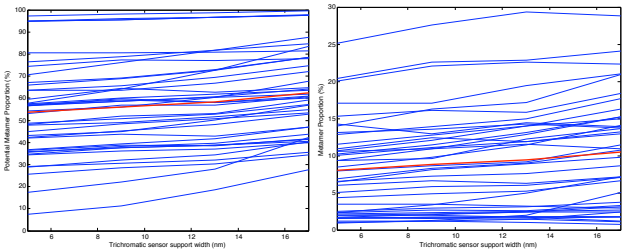

Figure 9. *The % of potential metamers in an image (left) and the % of actual metamers in an image (right) as a function of the width of trichromatic sensors for each of the 40 multi-spectal images (thin lines) as well as the average (bold lines).*

Conclusions

Metamerism and reflectance estimation are closely related and both depend to a large degree on device spectral sensitivity design. It has been argued on numerous occasions that increasing the number of sensors improves reflectance estimation accuracy and more recently, that narrow band sensors are better suited for the related task of discriminating reflectances. To this end however, no framework has been proposed to study device spectral sensitivity design from the point of view of metamerism.

In this paper we presented such a framework and showed results of analysing color input devices from the point of view of characterising their degree of metamerism. We expressed the degree of metamerism using three measures (proportion of potential metamers, proportion of actual metamers and magnitude of colour mismatch) and suggested a new way to visualise a device's degree of metamerism for a particular image.

Our results support both conclusions from the domain of reflectance estimation, that increasing the number of sensors reduces metamerism and that narrow band sensors also reduce metamerism, and provide means to express them quantitatively.

Acknowledgements

This research was partially funded by the Japan Society for the Promotion of Science (JSPS KAKENHI 1806703) as well as the National Institute of Information and Communications Technology (NICT) of Japan. Peter Morovic expresses his gratitude to Virginia Palacios and Jordi Arnabat of Hewlett Packard Company for their kind support.

References

[1] P. D. Burns and R. S. Berns. Analysis multispectral image capture. In *Proceedings of IS&T and SID's 4th Color Imaging Conference*, pages 19 – 22, 1996.

[2] M. S. Drew and B. V. Funt. Natural metamers. *CVGIP: Image Understanding*, pages 139–151, September 1992.

[3] D. Dupont. Study of the reconstruction of reflectance curves based on tristimulus values: Comparison of methods of optimization. *Color Research and Application*, 27, 2002.

[4] G. D. Finlayson, S. D. Hordley, and P. Morovic. Using the SpectraCube to build a multispectral image database. In *Proceedings of IS&T's 2nd European Conference on Colour Graphics, Imaging, and Vision*, pages 268 – 274, 2004.

[5] G. D. Finlayson and P. Morovic. Metamer sets. *Journal of the Optical Society of America A*, 22:810 – 819, 2005.

[6] D. H. Foster, K. Amano, S. M. C. Nascimento, and M. J. Foster. Frequency of metamerism in natural scenes. *Journal of the Optical Society of America A*, 6(10):2359 – 2372, 2006.

[7] J. Y. Hardeberg. *Acquisition and Reproduction of Colour Images: Colorimetric and Multispectral Approaches*. PhD. Thesis, Ecole Nationale Supérieure des Télécommunications, Paris, France, 1999.

[8] S. D. Hordley. *Colour constancy algorithms*. PhD thesis, Colour & Imaging Institute, University of Derby, 1999.

[9] E. H. Land. The retinex theory of color vision. *Scientific American*, 1977.

[10] C. Li and M. R. Luo. The estimation of spectral reflectances using the smoothest constraint condition. *IS&T/SID 9th Color Imaging Conference, Scottsdale, Arizona*, 2001.

[11] L. T. Maloney and B. A. Wandell. Color constancy: a method for recovering surface spectral reflectance. *Journal of the Optical Society of America A*, 3:29–33, 1986.

[12] P. Morovic and G. D. Finlayson. Metamer set based reflectance estimation. *Journal of the Optical Society of America A*, 23(8):1814–1822, 2006.

[13] P. Morovic and H. Haneishi. Estimating reflectances from multi-spectral video responses. In *IS&T and SID's 14th Color Imaging Conference*, 2006.

[14] P. Morovic and H. Haneishi. Quantitative analysis of metamerism for multispectral image capture. In *The 9th Internat. Symp. on Multispectral Colour Sci. and App.*, 2007.

[15] P. Morovic and H. Haneishi. A quantitative analysis of surface metamerism. In *The 2nd Internat. Workshop on Image Media Quality and its Apps.*, 2007.

[16] P. Morovic and J. Morovic. Spectral gamuts of inptu colour devices. In *IS&T and SID's 14th Color Imaging Conference*, 2006.

[17] S. M. C. Nascimento, F. P. Ferreira, and D. H. Foster. Statistics of spatial cone-excitation ratios in natural scenes. *Journal of the Optical Society of America A*, 19(8), 2002.

[18] S. M. C. Nascimento, D. H. Foster, and K. Amano. Psychophysical estimates of the number of spectral-reflectance basis functions needed to reproduce natural scenes. *Journal of the Optical Society of America A*, 22(6):1017 – 1022, 2004.

[19] M. Parmar and S. J. Reeves. Optimization of color filter sensitivity functions for color filter array based image acquisition. In *IS&T and SID's 14th Color Imaging Conference*, pages 96 – 101, 2006.

[20] R. Schettini and B. Baorlo. Estimating reflectance functions from tristimulus values. *Applied Signal Processing*, 3:104–115, 1996.

[21] J. Tajima and E. Niinomi. Two invariance properties on object color changes under daylights. In *IS&T and SID's 14th Color Imaging Conference*, pages 180–184, 2006.

[22] C. van Trigt. Metameric blacks and estimating reflectance. *Journal of the Optical Society of America A*, 11(3):1003–1024, March 1994.

Author Biography

Peter Morovič received his BSc degree in theoretical computer science from the School of Mathematics and Physics at the Comenius University in Bratislava (Slovakia) and his PhD degree in computing from the School of Computing Sciences at the University of East Anglia in Norwich (UK) in 2002. He is currently a colour science engineer with Hewlett-Packard in Barcelona, Spain.

Hideaki Haneishi received his M.S. degree in 1987 and his Ph.D. degree in 1990 from the Tokyo Institute of Technology, Japan. Since 1990, he has been working with the Department of Information and Computer Sciences, Chiba University, Chiba, Japan. He was a visiting research scientist at the Department of Radiology, University of Arizona, from 1995-1996. He is currently an associate professor at the Research Center for Frontier Medical Engineering, Chiba University. His research interests include color image processing, image reconstruction and medical image processing.